ACS APPLIED MATERIALS & INTERFACES

Research Article

www.acsami.org

Boronic Acid-Functionalized Core–Shell–Shell Magnetic Composite Microspheres for the Selective Enrichment of Glycoprotein

Miaorong Pan,[†] Yangfei Sun,[‡] Jin Zheng,[†] and Wuli Yang*[,†]

[†]State Key Laboratory of Molecular Engineering of Polymers and Department of Macromolecular Science, Fudan University, 220 Handan Road, Shanghai 200433, China

[‡]State Key Laboratory of Genetic Engineering and School of Life Sciences, Fudan University, 220 Handan Road, Shanghai 200433, China

ABSTRACT: In this work, core–shell–shell-structured boronic acid-functionalized magnetic composite microspheres Fe_3O_4@SiO_2@poly (methyl methacrylate-*co*-4-vinylphenylbornoic acid) (Fe_3O_4@SiO_2@P(MMA-*co*-VPBA)) with a uniform size and fine morphology were synthesized. Here, Fe_3O_4 magnetic particles were prepared by a solvothermal reaction, whereas the Fe_3O_4@SiO_2 microspheres with a core–shell structure were obtained by a sol–gel process. 3-(Trimethoxysilyl) propyl methacrylate (MPS)-modified Fe_3O_4@SiO_2 was used as the seed in the emulsion polymerization of MMA and VPBA to form the core–shell–shell-structured magnetic composite microspheres. As the boronic acid groups on the surface of Fe_3O_4@SiO_2@P(MMA-*co*-VPBA) could form tight yet reversible covalent bonds with the *cis*-1,2-diols groups of glycoproteins, the magnetic composite microspheres were applied to enrich a standard glycoprotein, horseradish peroxidase (HRP), and the results demonstrated that the composite microspheres have a higher affinity for the glycoproteins in the presence of the nonglycoprotein bovine serum albumin (BSA) over HRP. Additionally, different monomer mole ratios of MMA/VPBA were studied, and the results implied that using MMA as the major monomer could reduce the amount of VPBA with a similar glycoprotein enrichment efficiency but a lower cost.

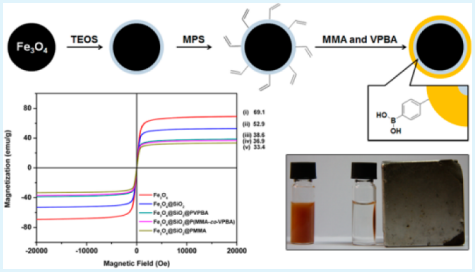

KEYWORDS: *magnetic particles, composite microspheres, core–shell, boronic acid, enrichment, glycoprotein*

1. INTRODUCTION

Glycoproteins are functional proteins with carbohydrates covalently connected to the side chains of the proteins. As an important post-translational modification of proteins in vivo, glycosylation contributes to diverse physiologic regulation in processes such as cell recognition, signal transduction, tumor immunology, inflammation, and so on.[1−4] Glycoprotein research has important biological significance and potential clinical applications. Mass spectrometry (MS) has been introduced into the study of glycoproteins to obtain detailed information on them, especially on the glycosylation-site occupancy and glycan heterogeneity at each glycol site.[5] However, the relatively low abundance (2−5%) of glycoproteins and their poor ionization efficiency often result in signal suppression in MS analysis.[6,7] It is necessary to enrich glycoproteins with specific and efficient methods in glycoproteomic studies.

Considering the typical structures and physicochemical properties of glycoproteins and glycopeptides, several enrichment strategies on the basis of lectins,[8−10] hydrazide chemistry,[11] hydrophilic interaction,[6,12−14] and size exclusion[15,16] have been developed. These methods are useful, but several limitations still need to be resolved. In recent decades, boronic acid derivatives have aroused more and more interest and have been studied widely in glycoprotein enrichment. The boronic acid groups can form a tight yet reversible covalent bond with glycoproteins containing *cis*-1,2-diols groups in an alkaline environment. What is important is that boronic acids are readily available, stabile, and versatile, complementing the above traditional methods to provide wider sugar-binding coverage and lower bias.[17,18]

Several materials immobilized with boronic acids have been reported for the solid-phase extraction of glycopeptides and glycoproteins. Boronic acid-based agarose resins provide quick, efficient, and specific enrichment of glycoproteins from complex samples such as human serum, and commercial *m*-aminophenylboronic acid-agarose resin has been widely used for glycoprotein enrichment and immobilization.[19−21] Mesoporous materials, which hold the attractive features of high surface area and large accessible porosity, such as mesoporous silica have been introduced into glycoprotein enrichment through the surface functionalization of boronic acids.[6] The monoliths functionalized with boronic acids also have been applied to glycoprotein separation for the versatile surface modification and better permeability along with a good peak capacity.[22−24] However, the steric and diffusive barriers between the boronic acid derivatives and solid-phase basis create an influence on the partial control of boronic acid

Received: April 8, 2013
Accepted: August 8, 2013
Published: August 8, 2013

conjugation during the grafting reaction. Recently, the core–shell-structured particles with a boronic acid-functionalized surface have been recognized as one of the more advanced strategies for this application because the copolymerization route employed presents obvious advantages that allow for better control of the yield of the grafted functional groups and the surface nature of the nanoparticles.[25,26] Qu and co-workers[27] reported polymer microspheres with a hydrophilic core and a boronic acid-functionalized shell, poly (*N*,*N*-methylenebisacrylamide-*co*-methacrylic acid)@poly (4-vinylphenylboronic acid) (P(MBA-*co*-MAA)@PVPBA). The boronic acid groups were introduced in the shell by free-radical polymerization rather than by employing a conventional solid–liquid heterogeneous grafting reaction. The microspheres were further applied to enrich glycosylated peptides for glycoproteome analysis with good selectivity.

Meanwhile, magnetic particles modified with boronic acids for glycoprotein enrichment have also attracted many researchers because of the fast separation of glycoprotein-conjugated magnetic materials from the sample solution because of the magnetic properties. For example, Zhou and co-workers[18] synthesized the aminophenylboronic acid-functionalized magnetic nanoparticles for glycoprotein enrichment through a two-step amidation reaction, and the particles achieved a rapid glycoprotein separation. However, less attention has been paid to adjusting the particle morphology, which might affect the efficiency of reaction and applications. Qi and co-workers[28] prepared Fe_3O_4@C@Au magnetic microspheres with a mercaptophenylboronic acid-functionalized shell. The core–shell-structured microspheres were successfully applied to the selective enrichment of glycoproteins, but the synthesis steps were complex, which might increase the cost of the experiment. Zhang and co-workers[29] synthesized the aminophenylboronic acid-functionalized magnetic mesoporous silica composites and successfully applied the composites to glycoprotein enrichment. A typical sandwich structure with a magnetite core, a nonporous silica layer in the middle layer, and an ordered mesoporous silica outer layer was prepared. The mesoporous silica layer offered a high surface area for the conjugation of boronic acid groups, but the remarkable size of the composites might limit the application of the particles and increase the cost of the material.

Herein, core–shell–shell-structured boronic acid-functionalized magnetic composite microspheres, Fe_3O_4@SiO_2@poly (methyl methacrylate-*co*-4-vinylphenylbornoic acid) (Fe_3O_4@SiO_2@P(MMA-*co*-VPBA)), were successfully synthesized via a seed-emulsion polymerization. The magnetic composite microspheres were composed of an almost uniform Fe_3O_4 core, providing a high magnetic response, a thin SiO_2 middle layer guaranteeing the conduction of subsequent reactions, and a polymer shell with boronic acid groups on the surface for selective glycoprotein enrichment. One of the cheapest boronic acid derivatives, 4-vinylphenylboronic acid (VPBA), was chosen as the reagent, and methyl methacrylate (MMA) was used as the main monomer to reduce further the amount of VPBA for lowering the cost. Such magnetic composite microspheres were successfully applied to glycoprotein enrichment.

2. EXPERIMENTAL SECTION

2.1. Materials. Iron(III) chloride anhydrous ($FeCl_3$), trisodium citrate dehydrate ($C_8H_5Na_3O_7{\cdot}2H_2O$), sodium acetate anhydrous (NaAc), ethylene glycol (EG), methyl methacrylate (MMA), styrene (St), tetraethyoxysilane (TEOS), aqueous ammonia solution (25 wt %), anhydrous ethanol, dodecyl sodium sulfate (SDS), potassium persulfate (KPS), and albumin from bovine serum (BSA, 98%, 66.4 kDa) were all purchased from Shanghai Chemical Reagents Company (China). MMA and St were purified through Al_2O_3 column, and KPS was recrystallized from water. 3-(Trimethoxysilyl) propyl methacrylate (MPS, 98%) was obtained from Acros Organics. Ethylene glycol dimethacrylate (EGDMA, 98%) and 4-vinylphenylbornoic acid (VPBA, 98%) were purchased from J&K Scientific Ltd. Horseradish peroxidase (HRP, RZ >2.0, activity >160 IU mg^{-1}, 44.0 kDa), myoglobin (MYO, 16.7 kDa), and cytochrome c (Cyt C, 12.3 kDa) were purchased from Aladdin Internet Reagent Database Inc., and phosphate-buffered saline (PBS) was obtained from the Shanghai Qiangshun Chemical Reagent Company. All reagents were of analytical grade or better.

2.2. Synthesis of Fe_3O_4 Magnetic Particles. The magnetic particles were prepared by the solvothermal reaction.[30] Briefly, 0.65 g of $FeCl_3$, 0.24 g of $C_8H_5Na_3O_7{\cdot}2H_2O$, and 1.2 g of NaAc were first dissolved in 20 mL of ethylene glycol under vigorous stirring for 30 min. The resulting solution was transferred into a Teflon-lined stainless steel autoclave with a capacity of 50 mL. The autoclave was sealed and heated at 200 °C for 10 h and then cooled to room temperature. The as-prepared black products were washed with ethanol and deionized water several times, collected with the help of a magnetic field, and vacuum-dried at 40 °C for 12 h.

2.3. Synthesis and Surface Modification of Fe_3O_4@SiO_2 Core–Shell Microspheres. Magnetic particles (250 mg) were dispersed in HNO_3 (0.1 M, 25 mL) and sonicated for 5 min. These products were washed with ethanol and deionized water and dispersed in a medium containing 100 mL of deionized water, 400 mL of ethanol, and 5 mL of aqueous ammonia (25 wt %). TEOS (10 mL) was added to the above dispersion under stirring. The dispersion was continuously stirred in a water bath (40 °C) for 6 h. Afterwards, the products were washed again with ethanol and deionized water to remove unreacted TEOS. To modify the surface of the Fe_3O_4@SiO_2 core–shell microspheres with MPS silane coupling agent, the core–shell microspheres were redispersed in a medium containing 100 mL of deionized water, 400 mL of ethanol, and 10 mL of aqueous ammonia (25 wt %). Next, 2.5 mL MPS was added. After mechanically stirring for 24 h at 60 °C, the Fe_3O_4@SiO_2-MPS core–shell microspheres were washed with ethanol with the help of a magnet and redispersed in 40 mL of ethanol for further use.

2.4. Synthesis of Fe_3O_4@SiO_2@P(MMA-*co*-VPBA) Magnetic Composite Microspheres. The core–shell–shell-structured Fe_3O_4@SiO_2@P(MMA-co-VPBA) magnetic composite microspheres were synthesized via seed-emulsion polymerization. Typically, in a three-necked round-bottomed flask (50 mL) equipped with a mechanical stirrer, a refluxing condenser, and a nitrogen inlet, 4 mL of an ethanol dispersion of Fe_3O_4@SiO_2-MPS core–shell microspheres was mixed with 30 mL of medium containing 6.0 mg of SDS under mechanically stirring. After stirring for 30 min, 0.5 mL of a KPS water solution (0.03 M) and 20 μL of EGDMA followed by 74 mg (0.5 mmol) of VPBA and 50 mg (0.5 mmol) of MMA were added to the dispersion, and the mixture was stirred vigorously for another 15 min. The flask was then immerged into a preheated oil bath at 75 °C, and the polymerization was carried out with a stirring speed of 200 rpm at 75 °C for 5 h. The resulting Fe_3O_4@SiO_2@P(MMA-*co*-VPBA) composite microspheres were harvested and washed by magnetic separation.

For the contrast test, Fe_3O_4@SiO_2@PVPBA and Fe_3O_4@SiO_2@PMMA were prepared with a similar procedure as that of Fe_3O_4@SiO_2@P(MMA-*co*-VPBA). After the addition of a KPS water solution and EGDMA, 148 mg (1.0 mmol) of VPBA and 100 mg (1.0 mmol) of MMA were added, respectively. The polymerization was then carried out under similar conditions as those above.

2.5. Enrichment of Glycoprotein HRP. The glycoprotein-enrichment behavior of the Fe_3O_4@SiO_2@P(MMA-*co*-VPBA) magnetic composite microspheres was studied in pH 5.0, 6.0, 7.4, 8.4, and 9.4 buffers. The glycoprotein HRP was first dissolved in buffer at a concentration of 0.1 mg mL^{-1}. Five milligrams of boronic acid-functionalized magnetic composite microspheres was dispersed in 2

Scheme 1. Scheme Illustrating the Synthesis Approach for the Preparation of the Boronic Acid-Functionalized Core–Shell–Shell Magnetic Composite Microspheres

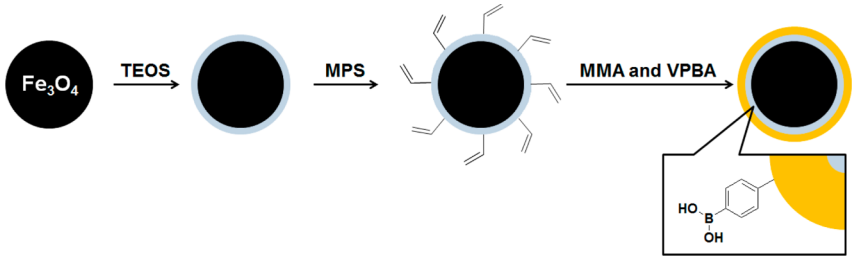

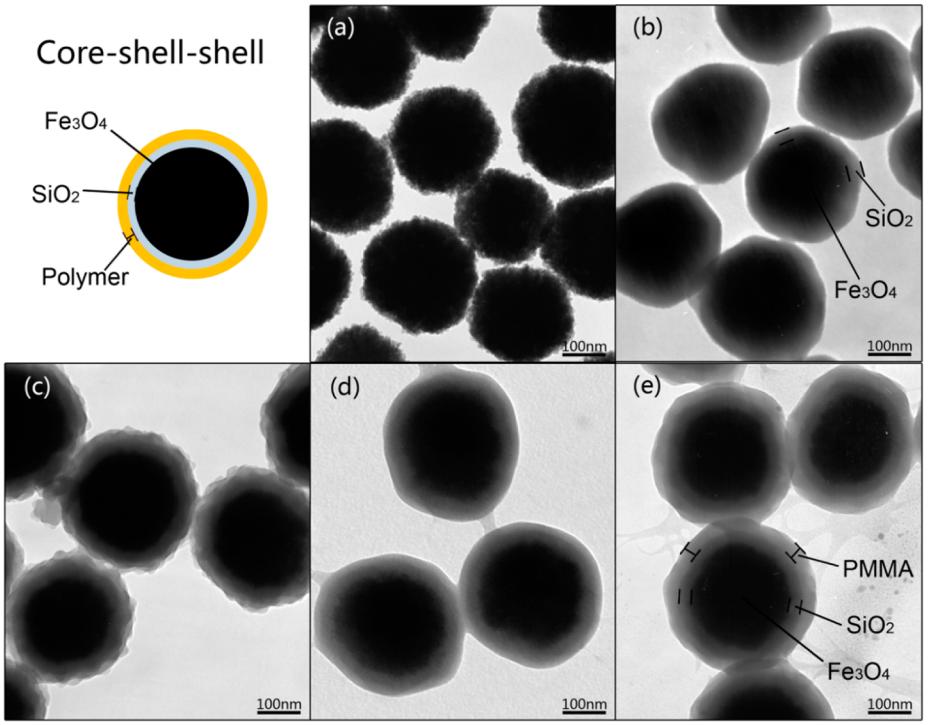

Figure 1. TEM images of (a) Fe_3O_4 magnetic particles, (b) Fe_3O_4@SiO_2 core–shell microspheres, (c) Fe_3O_4@SiO_2@PVPBA, (d) Fe_3O_4@SiO_2@P(MMA-*co*-VPBA), and (e) Fe_3O_4@SiO_2@PMMA magnetic composite microspheres. All scale bars are 100 nm.

mL of buffer. After sonication for 5 min, 0.5 mL of the HRP solution at the same pH was added to the mixture. Therefore, the weight ratio of the glycoprotein to the magnetic composite microspheres was 0.01, and the total volume of mixture was 2.5 mL. The resulting mixture was stirred at room temperature for 10, 20, 30, 40, 60, 120, and 240 min.

Afterwards, the HRP-enriched magnetic composite microspheres were collected by magnetic separation. The supernatant was kept for calculating the glycoprotein-enrichment content. The amount of HRP enriched on the magnetic composite microspheres was analyzed by UV at a wavelength of 405 nm.[31] The glycoprotein-enrichment content and enrichment efficiency were calculated using formulas 1 and 2, respectively:

$$\text{enrichment content (mg g}^{-1}) = \frac{\text{initial mass of HRP} - \text{supernatant free mass of HRP}}{\text{mass of magnetic composite microspheres}} \quad (1)$$

$$\text{enrichment efficiency (\%)} = \frac{\text{initial mass of HRP} - \text{supernatant free mass of HRP}}{\text{initial mass of HRP}} \times 100\% \quad (2)$$

2.6. Sodium Dodecyl Sulfate Polyacrylamide Gel Electrophoresis (SDS-PAGE) Analysis. The boronic acid-functionalized core–shell–shell magnetic composite microspheres were washed twice with pH 8.4 phosphate-buffered saline. Two-hundred microliters of a glycoprotein (1 μg μL^{-1}) and nonglycoprotein (1 μg μL^{-1}) mixture was treated with magnetic composite microspheres (about 20 mg) in a slightly alkaline (pH 8.4) buffer at room temperature under gentle stirring for 1 h. The magnetic composite microspheres were washed, and the glycoproteins were eluted under acidic conditions (pH 4). SDS-PAGE of the standard protein mixture, the raffinate, and the eluate was carried out according to Laemmli.[32] The proteins were separated by 10% SDS-polyacrylamide gels, and the protein bands were stained with Coomassie brilliant blue.

3. RESULTS AND DISCUSSION

The fabrication procedures for the boronic acid-functionalized core–shell–shell magnetic composite microspheres are schematically illustrated in Scheme 1. First, about 230 nm Fe_3O_4 magnetic particles were synthesized through a modified solvothermal reaction.[33] Second, the surface of the magnetic particles was coated a thin shell of dense amorphous silica.[34−36] The Fe_3O_4@SiO_2 core–shell microspheres were then modified with MPS to form an active C═C bond on the surface for the next polymerization. Finally, the second shell of polymer was coated on the Fe_3O_4@SiO_2-MPS by a seed-emulsion polymer-

dx.doi.org/10.1021/am401285x | ACS Appl. Mater. Interfaces 2013, 5, 8351−8358

ization of MMA and VPBA to synthesize the boronic acid-functionalized magnetic composite microspheres.

3.1. Preparation of the Boronic Acid-Functionalized Core–Shell–Shell Magnetic Composite Microspheres. Transmission electron microscopy (TEM) showed that the Fe_3O_4 magnetic particles were magnetite colloid nanocrystal clusters consisting of many small nanocrystals.[37] The obtained particles were nearly spherical in shape and had an average diameter of 230 ± 15 nm (Figure 1a). A typical TEM image of the obtained Fe_3O_4@SiO_2 core–shell microspheres showed that the dark magnetic particles were individually coated with a uniform gray silica shell (Figure 1b). After coating with a thin SiO_2 layer, the diameter of Fe_3O_4@SiO_2 increased to 280 ± 15 nm, corresponding to a 25 ± 5 nm thick SiO_2 layer on the Fe_3O_4 particles, and the surface of Fe_3O_4@SiO_2 became more smooth than that of the Fe_3O_4 magnetic particles. For the blank control, Fe_3O_4@SiO_2@PVPBA and Fe_3O_4@SiO_2@PMMA were also prepared as well as Fe_3O_4@SiO_2@P(MMA-*co*-VPBA). TEM images of the obtained Fe_3O_4@SiO_2@PVPBA (Figure 1c), Fe_3O_4@SiO_2@P(MMA-*co*-VPBA) (Figure 1d), and Fe_3O_4@SiO_2@PMMA (Figure 1e) showed that the expected composite microspheres with a core–shell–shell structure were all well obtained, which contained a dark Fe_3O_4 core, a gray SiO_2 middle layer, and a light-gray polymer shell of about 25 ± 5 nm in thickness. The clarity in the observation of this unique structure was due to the distinct mass contrast between these three components.[38] The images also revealed a relatively rough surface of Fe_3O_4@SiO_2@PVPBA and smooth surfaces of Fe_3O_4@SiO_2@P(MMA-co-VPBA) and Fe_3O_4@SiO_2@PMMA. The surface modifications of the Fe_3O_4@SiO_2 core–shell microspheres, Fe_3O_4@SiO_2@P(MMA-*co*-VPBA), and Fe_3O_4@SiO_2@PVPBA magnetic composite microspheres were investigated by X-ray photoelectron spectroscopy (XPS) (Table 1). Before coating with polymer, the percentage contents of Fe and Si were 0.6 and 12.6%, respectively. After coating with polymer, the Fe content disappeared, and the Si content decreased to 1.6%, whereas the percentage content of B turned out to be 2.7%, which revealed that the Fe_3O_4@SiO_2 core–shell microspheres had been well coated with the second shell of the copolymer of P(MMA-*co*-VPBA). Fe_3O_4@SiO_2@PVPBA also had similar changes in the percentage contents of Fe, Si, and B on the surface, suggesting that the second shell of PVPBA was coated on the Fe_3O_4@SiO_2 core–shell microspheres. Moreover, the contents of B on the core–shell–shell magnetic microspheres surface were close, which indicated a similar coating amount of boronic acid groups on the surface of both microspheres.

Table 1. Surface Element Percentage of Fe_3O_4@ SiO_2, Fe_3O_4@SiO_2@P(MMA-*co*-VPBA), and Fe_3O_4@SiO_2@ PVPBA Microspheres Analyzed by X-ray Photoelectron Spectroscopy

sample code	Fe (%)	Si (%)	B (%)
Fe_3O_4@SiO_2	0.6	12.6	
Fe_3O_4@SiO_2@P(MMA-*co*-VPBA)		1.6	2.7
Fe_3O_4@SiO_2@PVPBA		1.9	2.3

The functional groups of the microspheres surface were proved further by FT-IR. Figure 2 shows the FT-IR spectra of the Fe_3O_4 particles, Fe_3O_4@SiO_2 core–shell microspheres, Fe_3O_4@SiO_2@PVPBA, Fe_3O_4@SiO_2@P(MMA-*co*-VPBA), and Fe_3O_4@SiO_2@PMMA magnetic composite microspheres. The absorption peaks for the Fe_3O_4@SiO_2 core–shell microspheres at 1100 cm^{-1} were assigned to the Si–O–Si vibration, whereas the peaks around 1630 and 3430 cm^{-1} were attributed to the absorbed water and hydroxyl groups, respectively. As a result of the presence of large quantities of PVPBA at the surface of the composite microspheres after coating with PVPBA, the FT-IR spectrum of Fe_3O_4@SiO_2@PVPBA showed a strong peak at 1361 cm^{-1}, which was assigned to the B–C vibration.[18] Similarly, the spectrum of the Fe_3O_4@SiO_2@PMMA microspheres showed strong peaks at 1729 and 2960 cm^{-1}, which were associated with the ester C=O and C–H bonds of the repeating MMA units, respectively.[38] The spectrum of Fe_3O_4@SiO_2@P(MMA-*co*-VPBA) showed both characteristic absorption peaks at 1361 and 1729 cm^{-1} for the B–C and C=O bonds, confirming that Fe_3O_4@SiO_2 was coated with the polymer shell of P(MMA-*co*-VPBA).

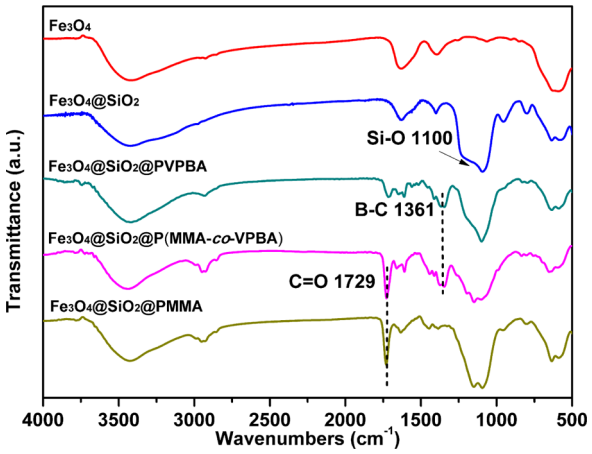

Figure 2. FT-IR spectra of Fe_3O_4, Fe_3O_4@SiO_2, Fe_3O_4@SiO_2@PVPBA, Fe_3O_4@SiO_2@P (MMA- *co*-VPBA), and Fe_3O_4@SiO_2@PMMA.

Thermogravimetric analysis (TGA) of Fe_3O_4@SiO_2, Fe_3O_4@SiO_2@PVPBA, Fe_3O_4@SiO_2@P(MMA-*co*-VPBA), and Fe_3O_4@SiO_2@PMMA was also performed (Figure 3). The TGA curves demonstrated that the weight loss of Fe_3O_4@SiO_2 was 8.3%, whereas the weight loss of Fe_3O_4@SiO_2@PVPBA, Fe_3O_4@SiO_2@P(MMA-*co*-VPBA), and Fe_3O_4@SiO_2@PMMA were 32.8, 36.2, and 45.0% at 800 °C, respectively. These

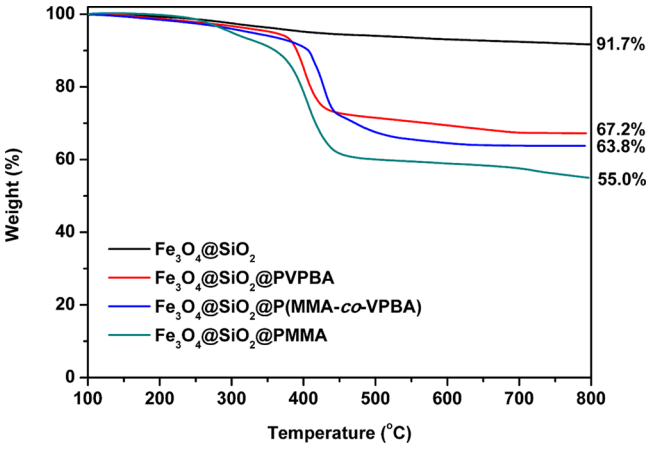

Figure 3. TGA curves of Fe_3O_4@SiO_2, Fe_3O_4@SiO_2@PVPBA, Fe_3O_4@SiO_2@P(MMA-*co*-VPBA), and Fe_3O_4@SiO_2@PMMA.

dx.doi.org/10.1021/am401285x | ACS Appl. Mater. Interfaces 2013, 5, 8351–8358

results agreed well with the scales of the core−shell−shell structure observed by TEM.

The magnetic properties of the Fe_3O_4 particles, Fe_3O_4@SiO_2 core−shell microspheres, Fe_3O_4@SiO_2@PVPBA, Fe_3O_4@SiO_2@P(MMA-*co*-VPBA), and Fe_3O_4@SiO_2@PMMA composite microspheres were determined with a vibrating sample magnetometer (VSM). The magnetic hysteresis curves are shown in Figure 4. The saturation magnetization value of Fe_3O_4 particles was 69.1 emu g^{-1}. After encapsulation with SiO_2, the saturation magnetization value was slightly reduced to 52.9 emu g^{-1}. After encapsulation with the second layer of the different polymers, the saturation magnetization value was significantly reduced to 38.6, 36.9, and 33.4 emu g^{-1} for Fe_3O_4@SiO_2@PVPBA, Fe_3O_4@SiO_2@P(MMA-*co*-VPBA), and Fe_3O_4@SiO_2@PMMA composite microspheres, respectively. These results indicated that the effective magnetic content in these composite microspheres were about 77, 56, 53, and 48% for Fe_3O_4@SiO_2, Fe_3O_4@SiO_2@PVPBA, Fe_3O_4@SiO_2@P(MMA-*co*-VPBA), and Fe_3O_4@SiO_2@PMMA, respectively, which was also consistent with the TGA results. Although the saturation magnetization value of the core−shell−shell magnetic composite microspheres decreased greatly compared with the original Fe_3O_4 particles, the magnetic property was still strong enough to ensure that the microspheres could be magnetically separated rapidly, as demonstrated by the inset photograph in Figure 4. All of the magnetic composite microspheres could be attracted to the side wall that was close to the magnet within 60 s. Because no hysteresis curve was observed in Figure 4, all of the four kinds of microspheres were superparamagnetic at 300 K.[35]

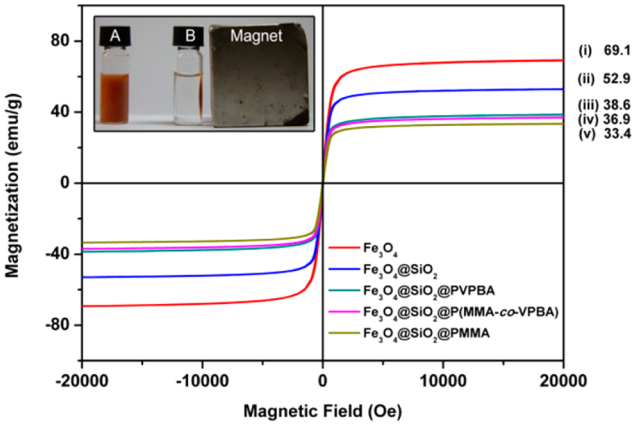

Figure 4. Magnetic hysteresis curves of (i) Fe_3O_4 magnetic particles, (ii) Fe_3O_4@SiO_2, (iii) Fe_3O_4@SiO_2@PVPBA, (iv) Fe_3O_4@SiO_2@P(MMA-*co*-VPBA), and (v) Fe_3O_4@SiO_2@PMMA microspheres at 300 K. The inset photograph shows two bottles of the sample Fe_3O_4@SiO_2@P(MMA-*co*-VPBA) with the same concentration of the aqueous solution in which the particles were (A) well-dispersed in water and (B) attracted to the side wall by a magnet. After slightly shaking, the particles could be dispersed again in water.

3.2. Glycoproteins Enrichment of the Boronic Acid-Functionalized Core−Shell−Shell Magnetic Composite Microspheres. The affinity between particles and glycoproteins is based on the typical boronate esterification reaction in which the boronic acid group reacts with *cis*-diols of glycans to form a cyclic ester in an alkaline aqueous medium, and these esters dissociate when the pH of the solution changes from neutral to acidic.[27] To characterize further the efficiency and selectivity of the as-synthesized boronic acid-functionalized core−shell−shell magnetic composite microspheres for glycoprotein enrichment, the Fe_3O_4@SiO_2@P(MMA-*co*-VPBA) magnetic composite microspheres were investigated by capturing the standard glycoprotein, horseradish peroxidase (HRP), under different stirring times and pH values. HRP has eight glycopeptides containing nine glycosylation sites,[39] which leads to a typical peak at 405 nm in the ultraviolet (UV) curve.[31] The amount of HRP enriched on the magnetic composite microspheres was analyzed by UV at the wavelength of 405 nm.

When Fe_3O_4@SiO_2@P(MMA-*co*-VPBA) magnetic composite microspheres were mixed with HRP in an aqueous dispersion at different pH (5, 6, 7.4, 8.4, and 9.4) values after 1 h of stirring and separation by a magnet, the enrichment content and efficiency were calculated from the supernatant. The results are shown in Table 2. The magnetic composite microspheres presented the relatively higher enrichment content and efficiency in alkaline solutions (7.63 mg g^{-1} and 77.5% at pH 8.4 and 7.48 mg g^{-1} and 75.9% at pH 9.4). When the pH was switched from neutral to acidic, the enrichment content and efficiency declined to approximately 5 mg g^{-1} and 50%, which corresponded to the equilibrium shift of the boronate esterification reaction caused by the reduction of the dissociated boronic anionic tetrahedral form in neutral and acidic aqueous systems.[40] The relation between the stirring time and HRP-enrichment efficiency was also investigated, and the results are shown in Table 3. The enrichment content and efficiency at pH 8.4 first increased sharply until 40 min (7.49 mg g^{-1} and 76.1%) and then flatted, which implied that the Fe_3O_4@SiO_2@P(MMA-*co*-VPBA) magnetic composite microspheres had a rapid enriching behavior in 40 min.

Table 2. Enrichment Content and Efficiency of Fe_3O_4@SiO_2@P(MMA-*co*-VPBA) Magnetic Composite Microspheres of HRP at Different Solution pH after 1 h of Stirring

pH	enrichment content (mg g^{-1})	enrichment efficiency (%)
5	5.10	50.6
6	4.76	48.2
7.4	5.35	53.8
8.4	7.63	77.5
9.4	7.48	75.9

Table 3. Enrichment Content and Efficiency of Fe_3O_4@SiO_2@P(MMA-*co*-VPBA) Magnetic Composite Microspheres of HRP after Different Amounts of Stirring Time at pH 8.4

stirring time (min)	enrichment content (mg g^{-1})	enrichment efficiency (%)
10	5.68	56.7
20	6.59	67.0
30	7.40	73.4
40	7.49	76.1
60	7.63	77.5
120	7.45	76.1
180	7.29	76.1

Because of the large volume of glycoprotein, the *cis*-1,2-diols groups of the glycoprotein mainly react with the boronic acid groups on the microspheres surface. The boronic acid groups

Table 4. Different Recipes[a] for the Preparation of Core−Shell−Shell Magnetic Composite Nanoparticles through Emulsifier-Free Emulsion Polymerization and the Corresponding HRP-Enriching Results at pH 8.4 after 1 h of Stirring

sample code	MMA (mg)	VPBA (mg)	enrichment content (mg g^{-1})	enrichment efficiency (%)
Fe_3O_4@SiO_2@PVPBA	0	148	7.16	69.9
Fe_3O_4@SiO_2@P(MMA-*co*-VPBA)-20[b]	20	118	7.52	75.3
Fe_3O_4@SiO_2@P(MMA-*co*-VPBA)-50	50	74	7.63	77.5
Fe_3O_4@SiO_2@P(MMA-*co*-VPBA)-80	80	29.6	7.46	74.3
Fe_3O_4@SiO_2@PMMA	100	0	1.02	10.2

[a]In these recipes, Fe_3O_4@SiO_2-MPS, 12.5 mg; EGDMA, 20 μL. [b]Suffix numbers refer to the mole percent of MMA, which corresponds to the total moles of MMA and VPBA.

embedded in the polymer shell may contribute less to the glycoprotein enrichment. Because boronic acid-carried monomers are expensive, whereas MMA has the merits of low cost, easy obtainment, and similar hydrophobicity with VPBA, the seed-emulsion polymerization introduced MMA as the comonomer to reduce the amount of VPBA, which might further lower the cost of the products. To estimate the influence of the VPBA content in the polymer shell on the glycoprotein enrichment, different recipes with a changing mole ratio of MMA/VPBA were followed (Table 4). The enrichment capability and efficiency that was investigated at a slight alkaline aqueous dispersion of pH 8.4 after 1 h are also shown in Table 4. After adding MMA, the enrichment capability and efficiency of the magnetic composite microspheres increased from 7.16 mg g^{-1} and 69.9% for Fe_3O_4@SiO_2@PVPBA to 7.52 mg g^{-1} and 75.3% for Fe_3O_4@SiO_2@P(MMA-*co*-VPBA)-20, 7.63 mg g^{-1} and 77.5% for Fe_3O_4@SiO_2@P(MMA-*co*-VPBA)-50, and 7.46 mg g^{-1} and 74.3% for Fe_3O_4@SiO_2@P(MMA-*co*-VPBA)-80, which implied that Fe_3O_4@SiO_2@P(MMA-*co*-VPBA) showed a slightly better glycoprotein-separation ability compared with Fe_3O_4@SiO_2@PVPBA and the reported work.[18] Additionally, as a hydrophobic polymer, PMMA has less nonspecific protein adsorption than that of other hydrophobic polymers such as polystyrene, which may lead to less influence on selective glycoprotein separation. When MMA completely replaced VPBA, the Fe_3O_4@SiO_2@PMMA microspheres had a much lower enrichment capability of 1.02 mg g^{-1} and an efficiency of 10.2%, which verified that PMMA has little nonspecific protein adsorption for HRP. For comparison, when MMA was replaced with styrene, the synthesized Fe_3O_4@SiO_2@PS had a higher enrichment capability (4.46 mg g^{-1}) and efficiency (45.4%) for HRP, which implied that PS has a stronger nonspecific protein adsorption.[41,42] The results were also confirmed by sodium dodecyl sulfate polyacrylamide gel electrophoresis (SDS-PAGE) analysis.

A protein mixture containing equivalent amounts of glycoprotein HRP (44.0 kDa) and nonglycoprotein BSA (66.4 kDa) was employed for the selective capture of glycoprotein. The particles were added into the protein mixture and stirred for 1 h at room temperature to ensure full contact between the proteins and particles. After being separated quickly by a magnet, the raffinate of the protein mixture was collected for the test, which might show some shade changes of the protein bands in the SDS-PAGE photographs that are related to the concentration changes of proteins. Meanwhile, the proteins-carried particles should be washed in the alkaline solution several times to wash away proteins absorbed by affinities other than the boronate esterification reaction. The glycoproteins enriched on the particles with the boronate esterification reaction were then eluted in an acidic solution. The eluate was detected to verify the glycoprotein separation ability of the particles. As shown in Figure 5, Fe_3O_4@SiO_2

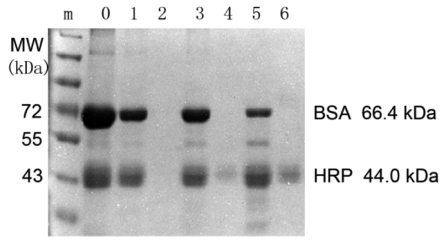

Figure 5. SDS-PAGE of a mixture of model proteins without treatment and the eluate after binding to the boronic acid-functionalized core−shell−shell magnetic composite microspheres. Lane m, marker; 0, mixture of HRP and BSA; 1 and 2, the raffinate and the eluate with treatment by Fe_3O_4@SiO_2, respectively; 3 and 4, the raffinate and the eluate with treatment by Fe_3O_4@SiO_2@PVPBA, respectively; and 5 and 6, the raffinate and the eluate with treatment by Fe_3O_4@SiO_2@P(MMA-*co*-VPBA), respectively.

(lanes 1 and 2) had almost no glycoprotein separation capability because their eluates demonstrated no protein band (lane 2), but both Fe_3O_4@SiO_2@PVPBA (lanes 3 and 4) and Fe_3O_4@SiO_2@P(MMA-*co*-VPBA) (lanes 5 and 6) could selectively enrich HRP. According to the dark level of the protein band, Fe_3O_4@SiO_2@P(MMA-*co*-VPBA) (lane 6) demonstrated more HRP than Fe_3O_4@SiO_2@PVPBA (lane 4) in the eluate. These microspheres were also successfully utilized to enrich HRP at a lower concentration of glycoprotein (HRP/BSA 1:10) in the protein mixture. At the same time, a more complex protein mixture of glycoprotein HRP mixed with equivalent nonglycoprotein BSA, myoglobin (MYO, 16.7 kDa), and cytochrome c (Cyt C, 12.3 kDa) was employed (Figure 6). After treatment with Fe_3O_4@SiO_2@P(MMA-*co*-VPBA), the raffinate (lane 1) still remained clear of the BSA, MYO, and Cyt C bands and had a lighter HRP band, whereas the eluate (lane 2) only showed an HRP band, suggesting that the glycoprotein can be selectively enriched from several nonglycoproteins in an complex mixture. Besides, other glycoproteins such as ovotransferrin (OVT) and ovalbvmin (OVA) have also been successfully enriched from a protein mixture with Fe_3O_4@SiO_2@P(MMA-*co*-VPBA). Because it forms reversible covalent bonds with the *cis*-diols of the glyco structure, the boronic acid groups can facilitate the enrichment of more kinds of N-linked and O-linked oligosaccharides[17,18] compared with lectins such as concanavalin A (ConA) that is mainly applied to capturing N-glycosylated peptides and proteins.[43,44]

Further study of Fe_3O_4@SiO_2@P(MMA-*co*-VPBA) with different monomer mole ratios of MMA/VPBA was conducted (Figure 7). The similar shade of the HRP bands in lanes 2, 4, and 6 implies that the three Fe_3O_4@SiO_2@P(MMA-*co*-VPBA)

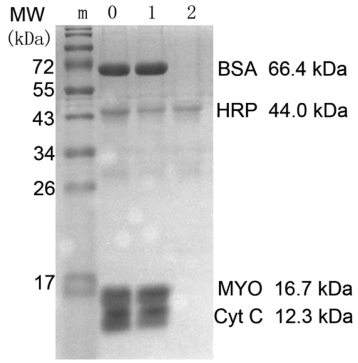

Figure 6. SDS-PAGE of a mixture of model proteins without treatment and the eluate after binding to the boronic acid-functionalized core–shell–shell magnetic composite microspheres. Lane m, marker; 0, mixture of BSA, MYO, Cyt C, and HRP; 1, the raffinate after treatment by Fe_3O_4@ SiO_2@P(MMA-*co*-VPBA); and 2, the eluate after treatment by Fe_3O_4@SiO_2@P(MMA-*co*-VPBA).

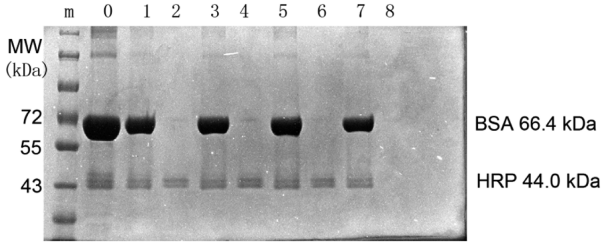

Figure 7. SDS-PAGE of a mixture of model proteins without treatment and the eluate after binding to the boronic acid-functionalized core–shell–shell magnetic composite microspheres. Lane m, marker; 0, mixture of HRP and BSA; 1 and 2, the raffinate and the eluate with treatment by Fe_3O_4@SiO_2@P(MMA-*co*-VPBA)-20; 3 and 4, the raffinate and the eluate with treatment by Fe_3O_4@SiO_2@P(MMA-*co*-VPBA)-50; 5 and 6, the raffinate and the eluate with treatment by Fe_3O_4@SiO_2@P(MMA-*co*-VPBA)-80; and 7 and 8, the raffinate and the eluate with treatment by Fe_3O_4@SiO_2@PMMA.

magnetic composite microspheres had similar good glycoprotein-enrichment behaviors. No protein band remained in the eluate (lane 8), revealing that Fe_3O_4@SiO_2@PMMA had almost no glycoprotein separation capability. All of these results confirmed the previous UV data. Hence, we can use MMA as the main monomer and VPBA as a minor monomer to form boronic acid-functionalized magnetic composite microspheres for selective glycoprotein enrichment at a rather low cost. Even the highest mole ratio of MMA/VPBA (80:20) could provide enough boronic acid groups on the microsphere surface for glycoprotein enrichment.

4. CONCLUSIONS

We have successfully synthesized core–shell–shell-structured boronic acid-functionalized Fe_3O_4@SiO_2@P(MMA-*co*-VPBA) magnetic composite microspheres via a seed-emulsion polymerization. The composite microspheres were composed of a magnetic core that provided a high magnetic response, an SiO_2 middle layer, and a polymer shell with boronic acid groups on the surface for the selective enrichment of glycoproteins. The magnetic composite microspheres were applied to the enrichment of the standard glycoprotein HRP, and the results demonstrated that the composite microspheres have a higher affinity for glycoproteins in the presence of the nonglycoprotein bovine serum albumin (BSA). Additionally, our results implied that using MMA as the major monomer could reduce the amount of VPBA and give a similar glycoprotein enrichment efficiency at a lower cost.

AUTHOR INFORMATION

Corresponding Author

*Tel: +86-21-65642385. Fax: +86-21-65640293. E-mail: wlyang@fudan.edu.cn.

Author Contributions

The manuscript was written through contributions of all authors. All authors have given approval to the final version of the manuscript.

Notes

The authors declare no competing financial interest.

ACKNOWLEDGMENTS

We are grateful for the support of the National Science Foundation of China (grant nos. 20874015 and 51273047), the Shanghai Rising-Star Program (10QH1400200), and the "Shu Guang" project (12SG07) supported by the Shanghai Municipal Education Commission and Shanghai Education Development Foundation.

REFERENCES

(1) Spiro, R. G. *Glycobiology* **2002**, *12*, 43R–56R.
(2) Dwek, M. V.; Ross, H. A.; Leathem, A. J. C. *Proteomics* **2001**, *1*, 756–762.
(3) Ireland, B. S.; Brockmeier, U.; Howe, C. M.; Elliott, T.; Williams, D. B. *Mol. Biol. Cell* **2008**, *19*, 2413–2423.
(4) Krishnamoorthy, L.; Mahal, L. K. *ACS Chem. Biol.* **2009**, *4*, 715–732.
(5) Kaji, H.; Saito, H.; Yamauchi, Y.; Shinkawa, T.; Taoka, M.; Hirabayashi, J.; Kasai, K.; Takahashi, N.; Isobe, T. *Nat. Biotechnol.* **2003**, *21*, 667–672.
(6) Xu, Y. W.; Wu, Z. X.; Zhang, L. J.; Lu, H. J.; Yang, P. Y.; Webley, P. A.; Zhao, D. Y. *Anal. Chem.* **2009**, *81*, 503–508.
(7) Dell, A.; Morris, H. R. *Science* **2001**, *291*, 2351–2356.
(8) Bunkenborg, J.; Pilch, B. J.; Podtelejnikov, A. V.; Wisniewski, J. R. *Proteomics* **2004**, *4*, 454–465.
(9) Hirabayashi, J. *Glycoconjugate J.* **2004**, *21*, 35–40.
(10) Cummings, R. D.; Kornfeld, S. *J. Biol. Chem.* **1982**, *257*, 1235–1240.
(11) Zhang, H.; Li, X. J.; Martin, D. B.; Aebersold, R. *Nat. Biotechnol.* **2003**, *21*, 660–666.
(12) Wada, Y.; Tajiri, M.; Yoshida, S. *Anal. Chem.* **2004**, *76*, 6560–6565.
(13) Yu, L.; Li, X.; Guo, Z.; Zhang, X.; Liang, X. *Chem.—Eur. J.* **2009**, *15*, 12618–12626.
(14) Selman, M. H. J.; Hemayatkar, M.; Deelder, A. M.; Wuhrer, M. *Anal. Chem.* **2011**, *83*, 2492–2499.
(15) Alvarez-Manilla, G.; Atwood, J.; Guo, Y.; Warren, N. L.; Orlando, R.; Pierce, M. *J. Proteome Res.* **2006**, *5*, 701–708.
(16) Zielinska, D. F.; Gnad, F.; Wisniewski, J. R.; Mann, M. *Cell* **2010**, *141*, 897–907.
(17) Sparbier, K.; Koch, S.; Kessler, I.; Wenzel, T.; Kostrzewa, M. *J. Biomol. Tech.* **2005**, *16*, 407–413.
(18) Zhou, W.; Yao, N.; Yao, G.; Deng, C.; Zhang, X.; Yang, P. *Chem. Commun.* **2008**, *43*, 5577–5579.
(19) Cartwright, S. J.; Waley, S. G. *Biochem. J.* **1984**, *221*, 505–512.
(20) Liu, X. C.; Scouten, W. H. *J. Mol. Recognit.* **1996**, *9*, 462–467.
(21) Bhatnagar, P. K.; Das, D.; Suresh, M. R. *J. Chromatogr., B* **2008**, *863*, 235–241.
(22) Sun, X. L.; Liu, R.; He, X. W.; Chen, L. X.; Zhang, Y. K. *Talanta* **2010**, *81*, 856–864.
(23) Yang, F.; Lin, Z. A.; He, X. W.; Chen, L. X.; Zhang, Y. K. *J. Chromatogr., A* **2011**, *1218*, 9194–9201.

(24) Lin, Z. A.; Pang, J. L.; Yang, H. H.; Cai, Z. W.; Zhang, L.; Chen, G. N. *Chem. Commun.* **2011**, *47*, 9675−9677.
(25) Qi, D. L.; Yang, X. L.; Huang, W. Q. *Polym. Int.* **2007**, *56*, 208−213.
(26) Li, W. H.; Stover, H. D. H. *Macromolecules* **2000**, *33*, 4354−4360.
(27) Qu, Y. Y.; Liu, J. X.; Yang, K. G.; Liang, Z.; Zhang, L. H.; Zhang, Y. K. *Chem.—Eur. J.* **2012**, *18*, 9056−9062.
(28) Qi, D. W.; Zhang, H. Y.; Tang, J.; Deng, C. H.; Zhang, X. M. *J. Phys. Chem. C* **2010**, *114*, 9221−9226.
(29) Zhang, H. Y.; Yao, G. P.; Deng, C. H.; Lu, H. J.; Yang, P. Y. *Chin. J. Chem.* **2011**, *29*, 835−839.
(30) Ma, W. F.; Xu, S. A.; Li, J. M.; Guo, J.; Lin, Y.; Wang, C. C. *J. Polym. Sci., Part A: Polym. Chem.* **2011**, *49*, 2725−2733.
(31) Hofmann, S.; Foo, C.; Rossetti, F.; Textor, M.; Vunjak-Novakovic, G.; Kaplan, D. L.; Merkle, H. P.; Meinel, L. *J. Controlled Release* **2006**, *111*, 219−227.
(32) Laemmli, U. K. *Nature* **1970**, *227*, 680−685.
(33) Xuan, S. H.; Wang, Y. X. J.; Yu, J. C.; Leung, K. C. F. *Chem. Mater.* **2009**, *21*, 5079−5087.
(34) Gao, R. X.; Kong, X.; Wang, X.; He, X. W.; Chen, L. X.; Zhang, Y. K. *J. Mater. Chem.* **2011**, *21*, 17863−17871.
(35) Deng, H.; Li, X. L.; Peng, Q.; Wang, X.; Chen, J. P.; Li, Y. D. *Angew. Chem., Int. Ed.* **2005**, *44*, 2782−2785.
(36) Xu, X.; Deng, C.; Gao, M.; Yu, W.; Yang, P.; Zhang, X. *Adv. Mater.* **2006**, *18*, 3289−3293.
(37) Liu, J.; Sun, Z. K.; Deng, Y. H.; Zou, Y.; Li, C. Y.; Guo, X. H.; Xiong, L. Q.; Gao, Y.; Li, F. Y.; Zhao, D. Y. *Angew. Chem., Int. Ed.* **2009**, *48*, 5875−5879.
(38) Chen, H.; Deng, C.; Zhang, X. *Angew. Chem., Int. Ed.* **2010**, *49*, 607−611.
(39) Qi, D.; Zhang, H.; Tang, J.; Deng, C.; Zhang, X. *J. Phys. Chem. C* **2010**, *114*, 9221−9226.
(40) Cambre, J. N.; Sumerlin, B. S. *Polymer* **2011**, *52*, 4631−4643.
(41) De Sousa Delgado, A.; Leonard, M.; Dellacherie, E. *Langmuir* **2001**, *17*, 4386−4391.
(42) Reimhult, K.; Petersson, K.; Krozer, A. *Langmuir* **2008**, *24*, 8695−8700.
(43) Sparbier, K.; Wenzel, T.; Kostrzewa, M. *J. Chromatogr., B* **2006**, *840*, 29−36.
(44) Tang, J.; Liu, Y.; Yin, P.; Yao, G.; Yan, G.; Deng, C.; Zhang, X. *Proteomics* **2010**, *10*, 2000−2014.